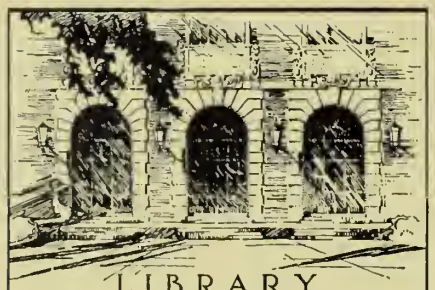

Antenna Laboratory

Technical Report No. 11

A TECHNIQUE FOR CONTROLLING THE RADIATION FROM DIELECTRIC ROD WAVEGUIDES

by

J. W. Duncan
R. H. DuHamel

15 July 1956

Contract AF33(616)-3220
Project No. 6(7-4600)Task 40572
WRIGHT AIR DEVELOPMENT CENTER

Electrical Engineering Research Laboratory
Engineering Experiment Station
University of Illinois
Urbana, Illinois

ABSTRACT

This paper describes a technique for controlling the radiation from a dielectric rod waveguide by placing obstacles or antenna elements at appropriate points along the waveguide. The HE_{11} mode on a dielectric rod was used to excite concentric rings and slots, and radial wires. The coupling of the obstacles to the HE_{11} mode was determined by constructing an image line with a slotted section for impedance measurements. This information was used to design several antenna arrays with different types of patterns. The measured patterns were very satisfactory.

CONTENTS

ILLUSTRATIONS

1. INTRODUCTION

During recent years, increasing use has been made of surface wave antennas. Examples are corrugated surfaces, dielectric rods and tubes, dielectric coated conductors, dielectric slabs, etc. Most surface wave antennas have been designed for endfire or near endfire radiation. Only minor success has been obtained in controlling the radiation from surface wave antennas in directions other than endfire. The objective of this work has been to devise methods of modifying surface waveguides in such a manner that accurate control of the radiation can be obtained.

Mueller[1] succeeded in obtaining broadside radiation from a dielectric rod antenna by means of placing dielectric disks on the rod with approximately half-wavelength spacing between the disks. Although his simple array theory predicted the direction and width of the main beam with fair accuracy, control of the side lobe level could be obtained only on an empirical basis. A disadvantage of the dielectric disks was that the polarization was a function of the circumferential angle.

It is believed that the technique described in this paper will allow accurate designs of modified surface wave antennas. The method is similar to Mueller's in that obstacles or discontinuities are placed at appropriate points along the waveguide in order to force and control the radiation. If an obstacle, such as a piece of metal, is placed near an excited surface waveguide, it will radiate and will also excite surface waves. By choosing the proper waveguide dimensions and/or choosing obstacles with a certain symmetry, all surface wave modes except one may be made negligible. The antenna system may then be represented by a single transmission line loaded at the appropriate point by the equivalent obstacle four-pole network. If the axial length of the obstacle is small, its equivalent admittance is a simple shunt element. Knowledge of the radiation pattern and the equivalent admittance of the obstacle would allow a simple, straightforward design of arrays of the obstacles to produce specified patterns. In some cases it may also be necessary to take into account the effect of the mutual admittance between the obstacles.

Briefly, the work to be described is the following: The coupling of wires, rings, and slots to the HE_{11} mode on a dielectric rod waveguide was measured. This information was then used to design several arrays to produce various types of patterns. The arrays were constructed and

tested. Good agreement between the predicted and measured patterns was obtained. Finally, the excitation efficiencies of several types of surface wave exciters were compared.

2. THE DIELECTRIC ROD WAVEGUIDE

The dominant HE_{11} (or dipole) mode on a dielectric rod is a hybrid mode which has axial components of both the electric and magnetic field intensities, and is unsymmetrical in that all field components vary as the sine or cosine of the circumferential angle, θ. The electric field configuration of the HE_{11} mode on a dielectric rod is shown in Fig. 1. The cutoff wavelength of a particular mode on the dielectric rod is a function of the rod radius, b, and the operating frequency or wavelength, λ. Characteristic curves showing the variation of λ_g/λ, the ratio of the

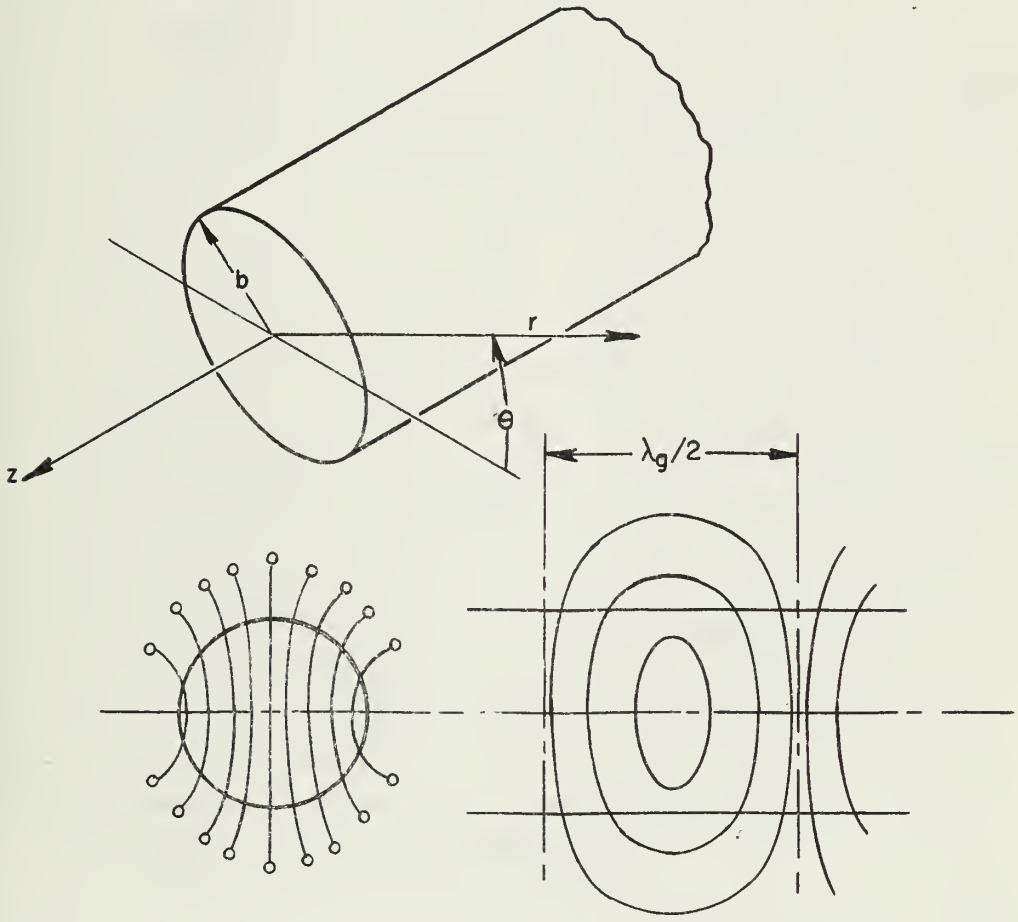

Figure 1 Approximate Electric Field Configuration of the HE_{11} Mode on a Dielectric Rod Waveguide (From Reference 2)

guide wavelength to the operating wavelength as a function of the parameter b/λ are plotted in Fig. 2. The curves are for the symmetrical E_{01}, H_{01}, E_{02}, and H_{02} modes, and the unsymmetrical HE_{11}, HE_{12}, and EH_{12} modes. The symmetrical modes on a dielectric rod are either transverse electric or transverse magnetic and the field intensities are independent of the angle θ.

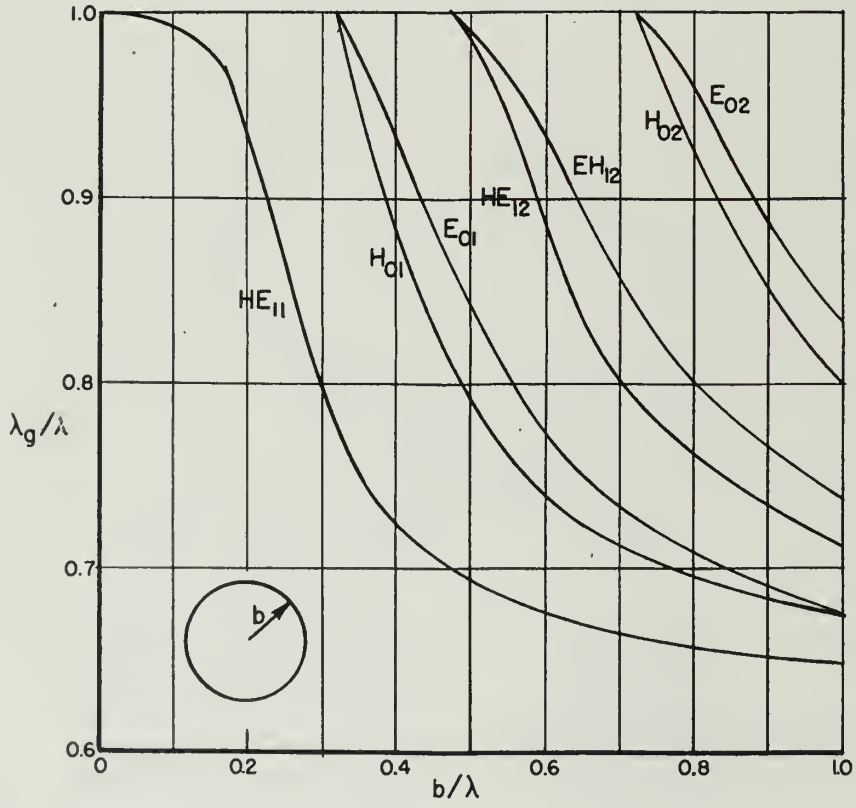

Figure 2. Characteristic Curves for Symmetrical and Unsymmetrical or Hybrid Modes on a Dielectric Rod (From Reference 2)

3. MEASUREMENT OF THE OBSTACLE ADMITTANCE

The dielectric rod waveguide was utilized to investigate modified surface wave antennas for two reasons. First, the rod has a simple geometry for which theoretical solutions are available. Second, by using an image system, accurate standing wave measurements may be made along the rod by means of a slotted section in the ground plane. Figure 3 illustrates the arrangement of equipment which was used to measure the equivalent shunt admittance of the various types of obstacles. Figure 4 is a photograph of the microwave equipment and dielectric image line. Shown from left to right are the signal oscillator and associated rectangular waveguide test equipment, the horn exciter, the dielectric rod image line, a ring type of obstacle, and a short circuit plate. The launching horn is a half-conical horn approximately 25.4 centimeters long with a mouth diameter of 17.8 centimeters. It is fed by a 16.2 centimeter length of half-cylindrical waveguide. The launching horn and dielectric rod are mounted on a 0.64 centimeter brass plate which is 206 centimeters long and 25.4 centimeters wide. Utilizing the image principle, the polystyrene rod has been halved along its length and fastened to the brass plane by polystyrene pins. The total length of the dielectric image line was approximately 168 centimeters for most of the admittance measurements. The polystyrene pins are 0.32 centimeter in diameter and two pins are used for each 28 centimeter section of rod. The rod sections were machined to accurate length to realize a very tight fit between the interface of two sections and thereby minimize reflections from the discontinuity of the interface. Measurements indicated that reflections from such discontinuities were negligible. The polystyrene rod has a diameter of 2.22 cm and the operating wavelength was maintained near 4.5 cm. This results in a b/λ ratio of about 0.25 and reference to Fig. 2 shows that the guide wavelength of the HE_{11} mode was approximately 86% of the operating or free space wavelength. The rod diameter and operating wavelength were purposely selected so that only the dominant HE_{11} mode was present on the rod waveguide; all higher order modes were cut off, as may be seen from Fig. 2. The short circuit plate is silver plated brass and has a radius of 4.45 centimeters.

The slotted section of the ground plane, which is located to the left of the ring obstacle, is shown in Fig. 5. The tapered slot is approximately 0.32 centimeter wide and 22.9 centimeters long. The probe

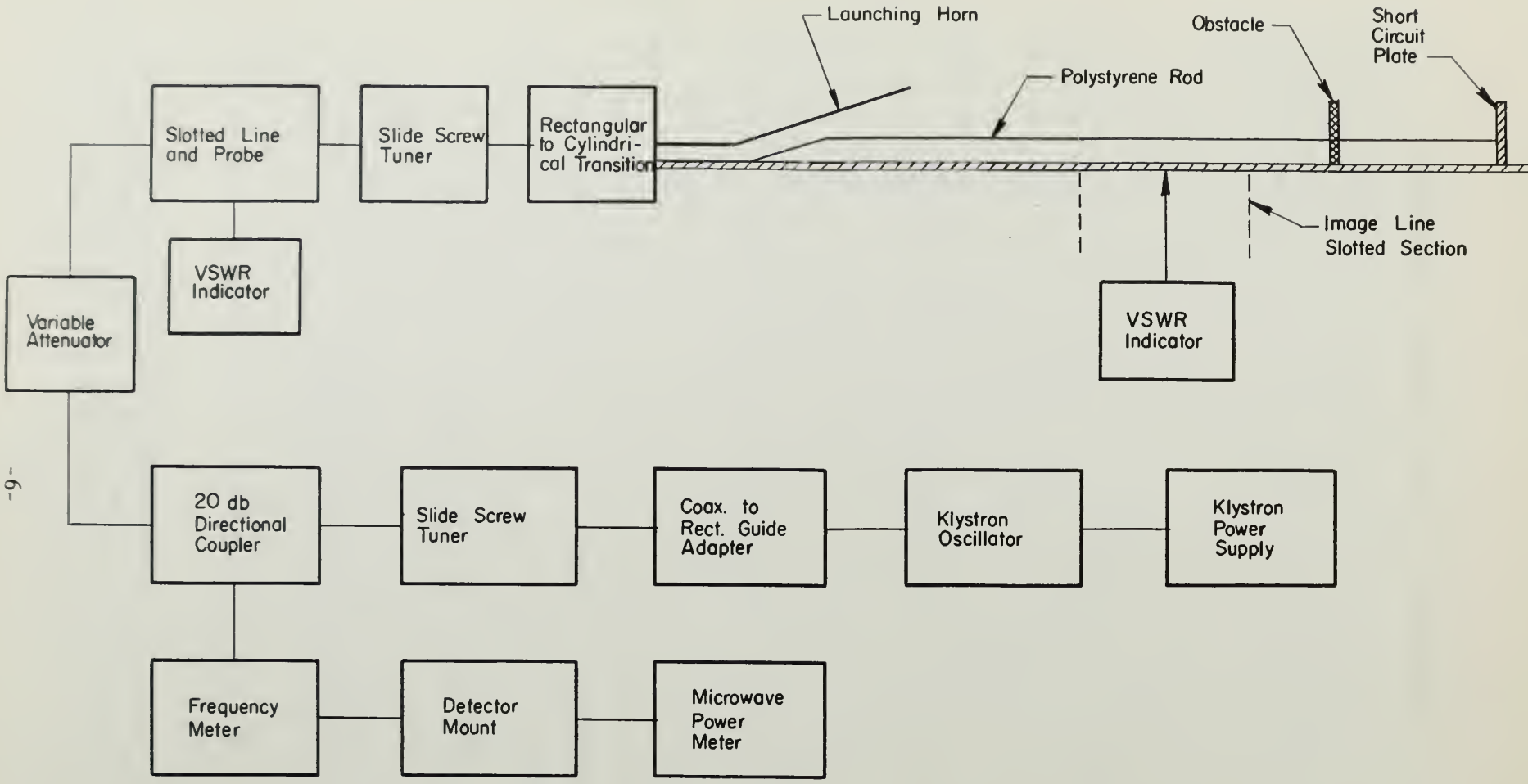

Figure 3. Diagram of the Equipment Used to Measure Obstacle Admittance

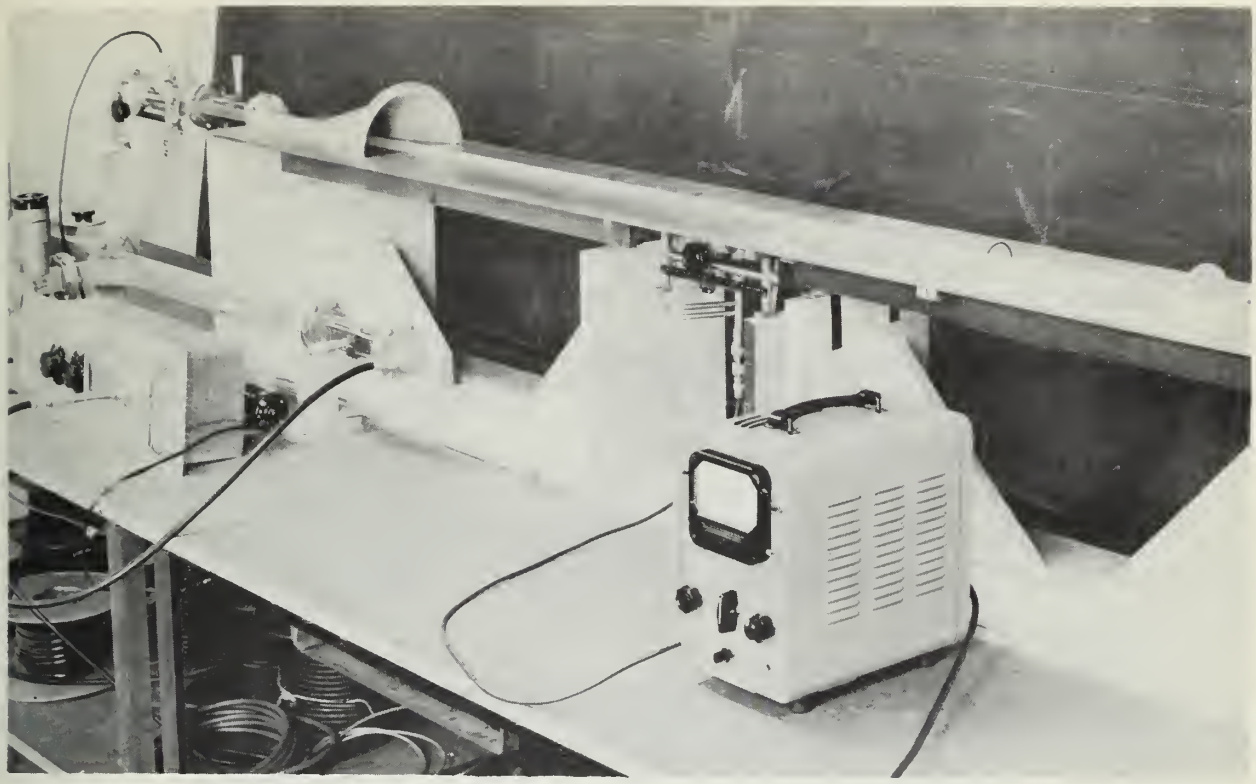

Figure 4. Apparatus for Measuring the Coupling of Obstacles to the Dielectric Rod Waveguide

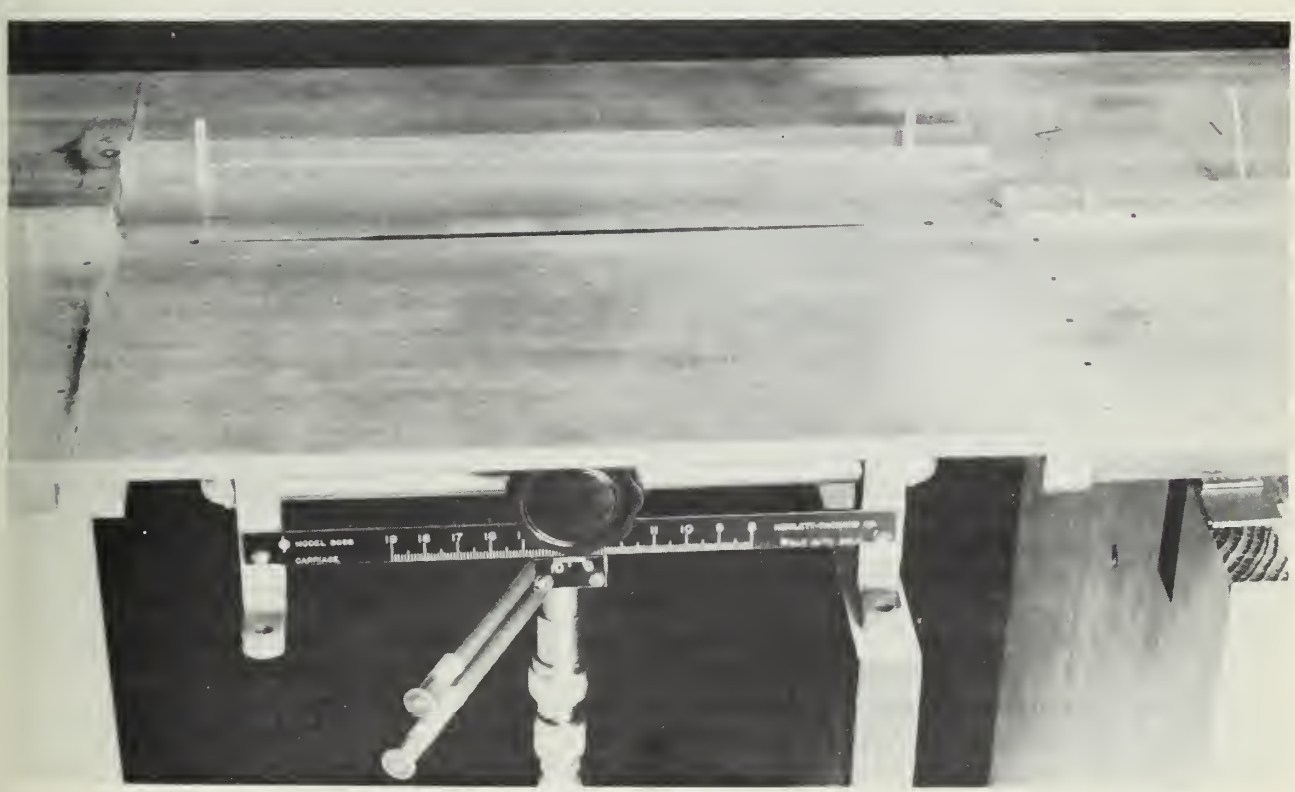

Figure 5. The Slotted Section

is supported by a Hewlett-Packard Universal Probe Carriage which was modified and mounted on the underside of the brass plate. An inclined wire obstacle may be seen on the right side of the picture. The operation of the slotted section was quite satisfactory. The residual VSWR was less than 0.2 db and VSWR's of 40 db were obtained for the line terminated with the short circuit plate.

Concentric rings and slots were placed on the image line by means of the plates shown in Fig. 6. The obstacles were fabricated from 0.08 centimeter brass plate. These plates were inserted at a break in the ground plane (see Fig. 4) and the two sections of the ground plane were then clamped to make good electrical contact. The slots were investigated to determine their usefulness as surface wave exciters.

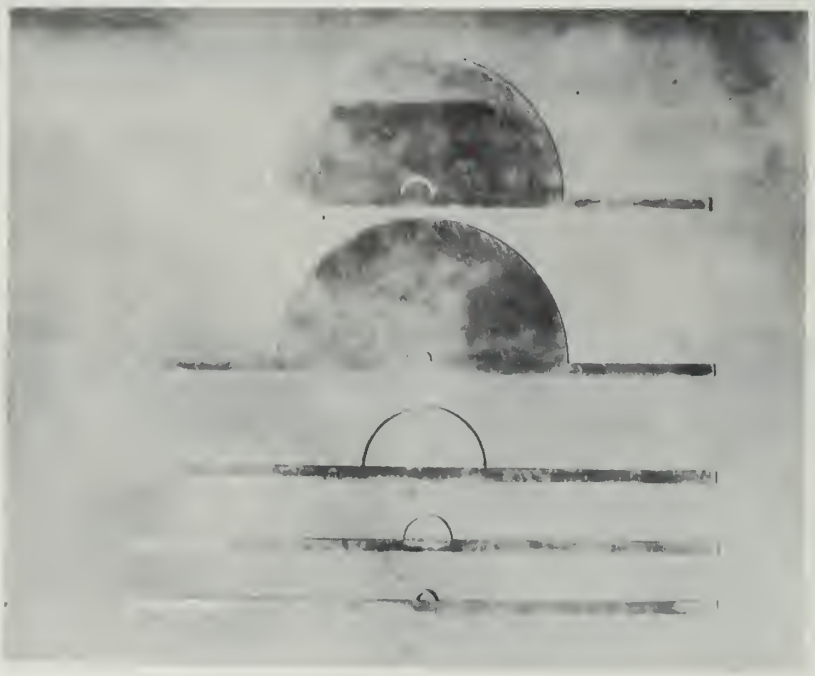

Figure 6. Slots and Rings for the Image Line

Since the existence of only a single mode was demonstrated, the admittance measurements were made in the same manner as that for a conventional waveguide and slotted section. The short circuit plate was always placed an odd number of quarter-wavelengths past the obstacle. The measured normalized shunt admittance of a ring as a function of the mean ring radius is presented in Fig. 7. Since the maximum VSWR that could be obtained with a short circuit termination was 29 db for the ring measurements, the points at the top of the

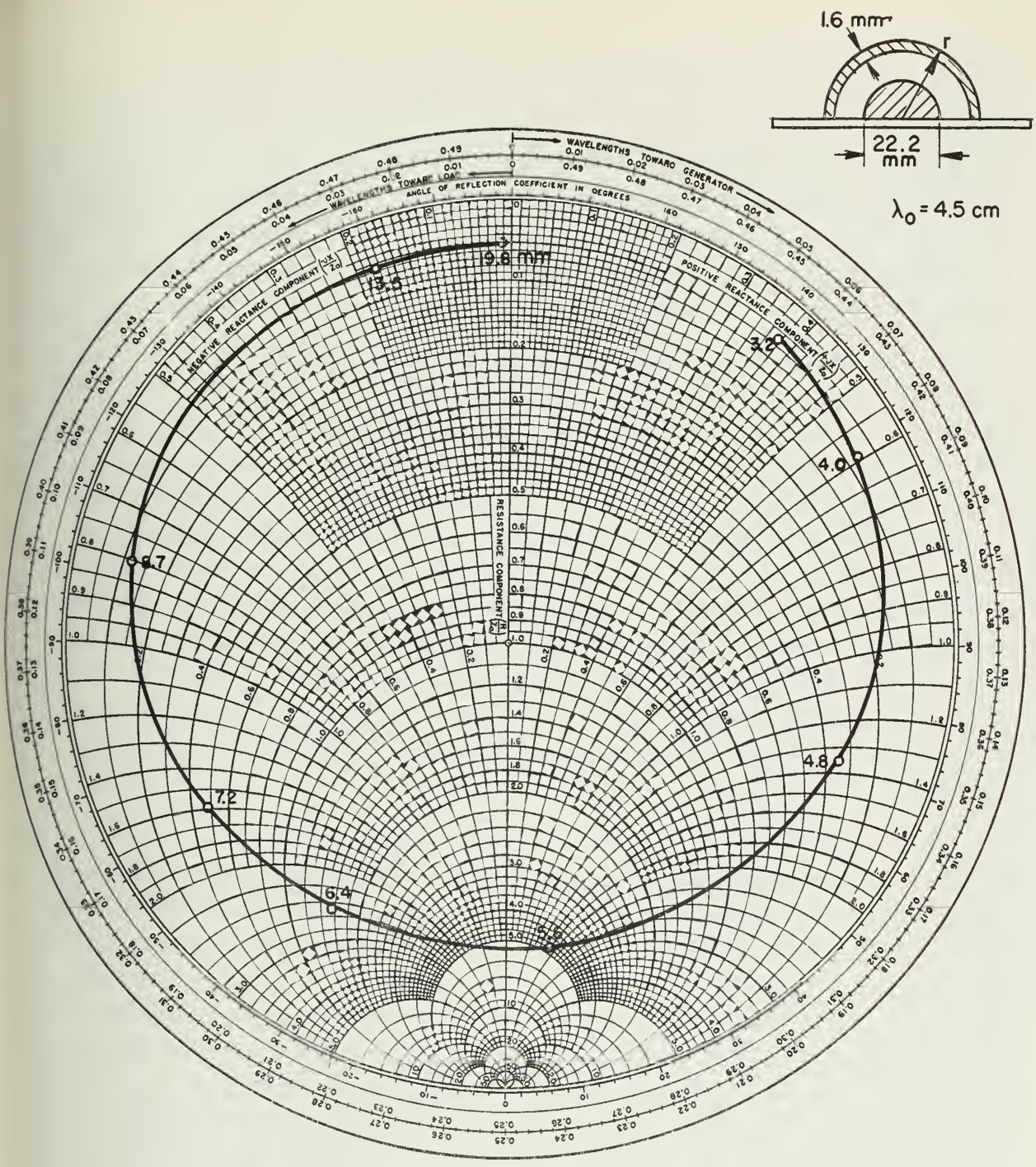

Figure 7 Shunt Admittance of a Ring as a Function of the Mean Ring Radius

admittance chart are not very accurate. Figure 8 shows the normalized shunt admittance of a slot as a function of the mean slot radius. Figure 9 shows the normalized shunt admittance of a vertical wire or monopole as a function of the wire length. For this series of measurements a VSWR of 40 db could be attained for short circuit termination of the line. It may be seen from Figs. 7 and 9 that the resonant ring and wire are strongly coupled to the line (conductances of 5.3 and 3.3, respectively).

In the design of an array it is certainly desirable, although not essential, to use resonant obstacles. In addition, the elements should be loosely coupled to the line, i.e., the conductance should be considerably less than one. It is readily seen that the ring and protruding wire do not satisfy these requirements. A study of the field distribution of the HE_{11} mode makes apparent two methods of controlling the coupling of resonant obstacles to the rod. First, since the fields decay exponentially away from the rod, a resonant obstacle could be displaced from the rod to reduce the coupling. Second, since the fields vary sinusoidally with the circumferential angle, certain types of resonant obstacles, such as wires, could be oriented or rotated about the axis of the guide to control the coupling. The work to be described below illustrates these methods

In Fig. 10 there is plotted the normalized shunt admittance of a wire normal to and displaced 3 mm from the slab as a function of the wire length For these and the following measurements the VSWR on the line with the short circuit plate was at least 37 db. Thus the points near the top of the chart are more accurate than some of those shown previously. The wire passed through the first and second resonances when its length was 0.38λ and 0.72λ, respectively. This measurement was repeated for two other displacements from which the curves of Fig. 11 were constructed. These curves show the normalized shunt conductance of the resonant wires as a function of the spacing from the ground plane Although control of the conductance has been obtained, it is apparent that the wire would have to be placed completely outside of the rod in order to obtain conductances of 0.1 or less. Additional support of the wire would then have to be provided.

Figure 12 shows the normalized admittance loci of an inclined wire as a function of the wire length for several angles of inclination This data was used to construct the curves of Fig. 13, which show the normalized shunt conductance of a resonant wire as a function of the

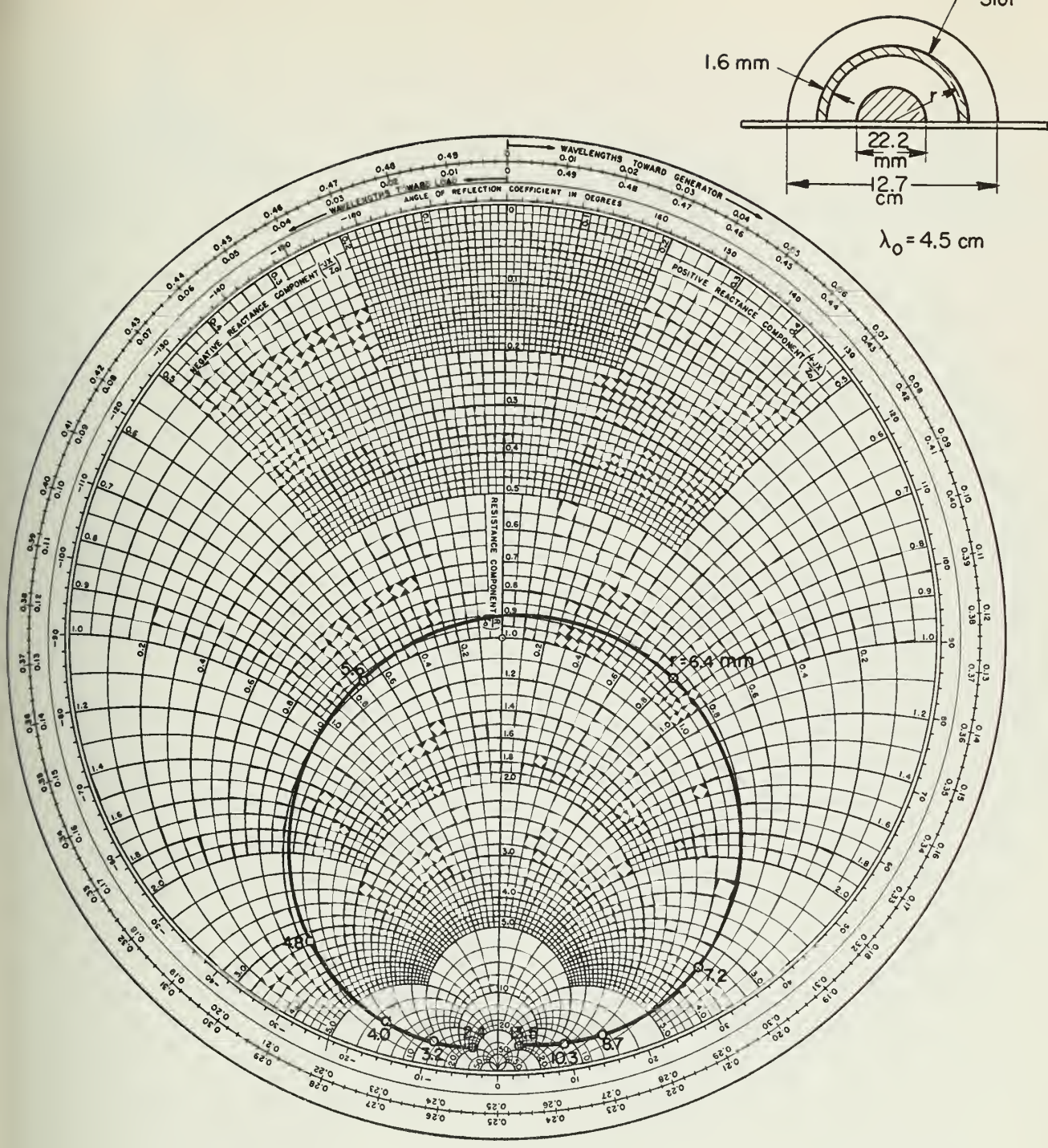

Figure 8. Shunt Admittance of a Slot as a Function of the Mean Slot Radius

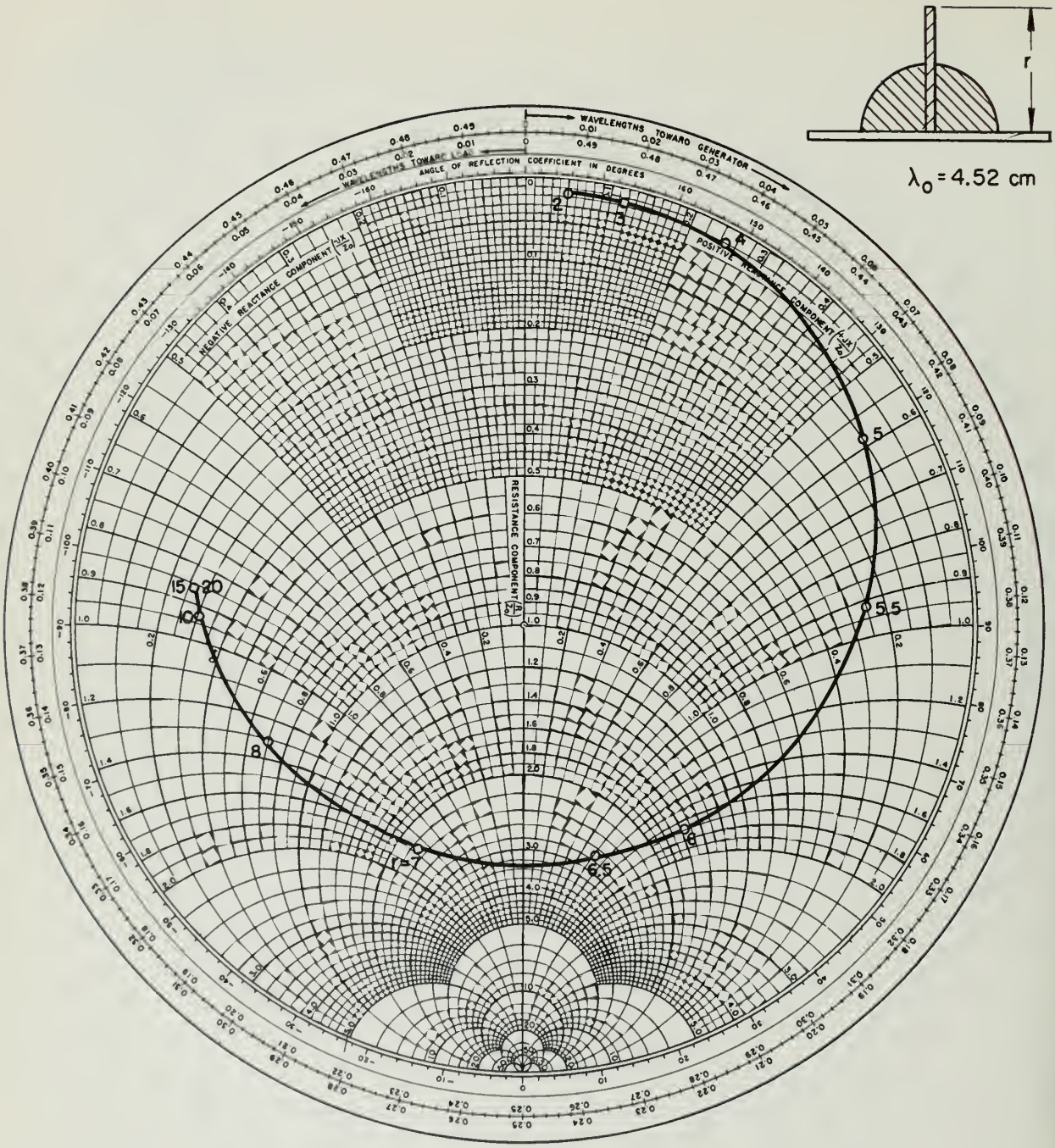

Figure 9 Shunt Admittance of a Vertical Wire as a Function of the Wire Length

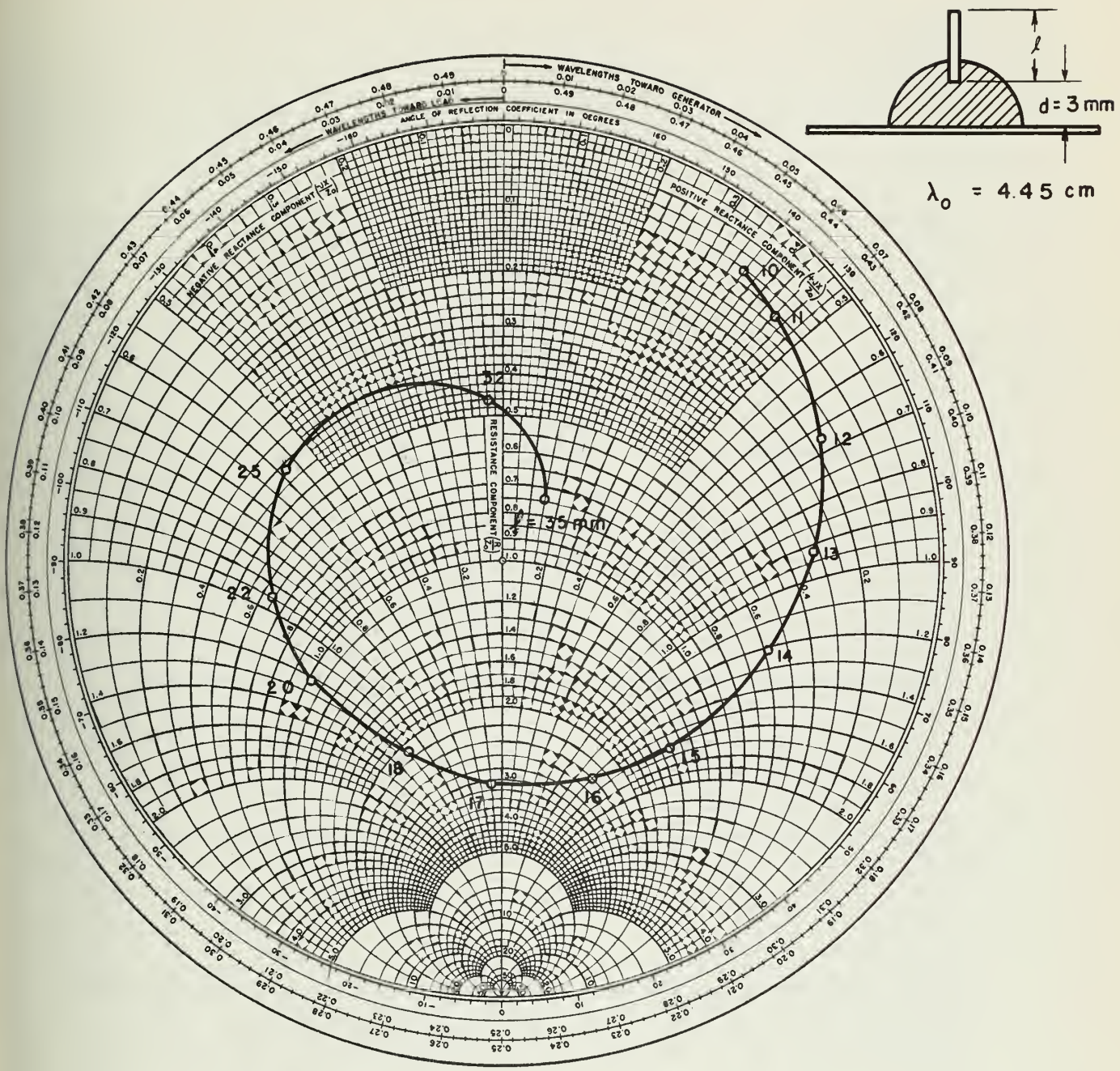

Figure 10. Shunt Admittance of a Wire as a Function of the Wire Length

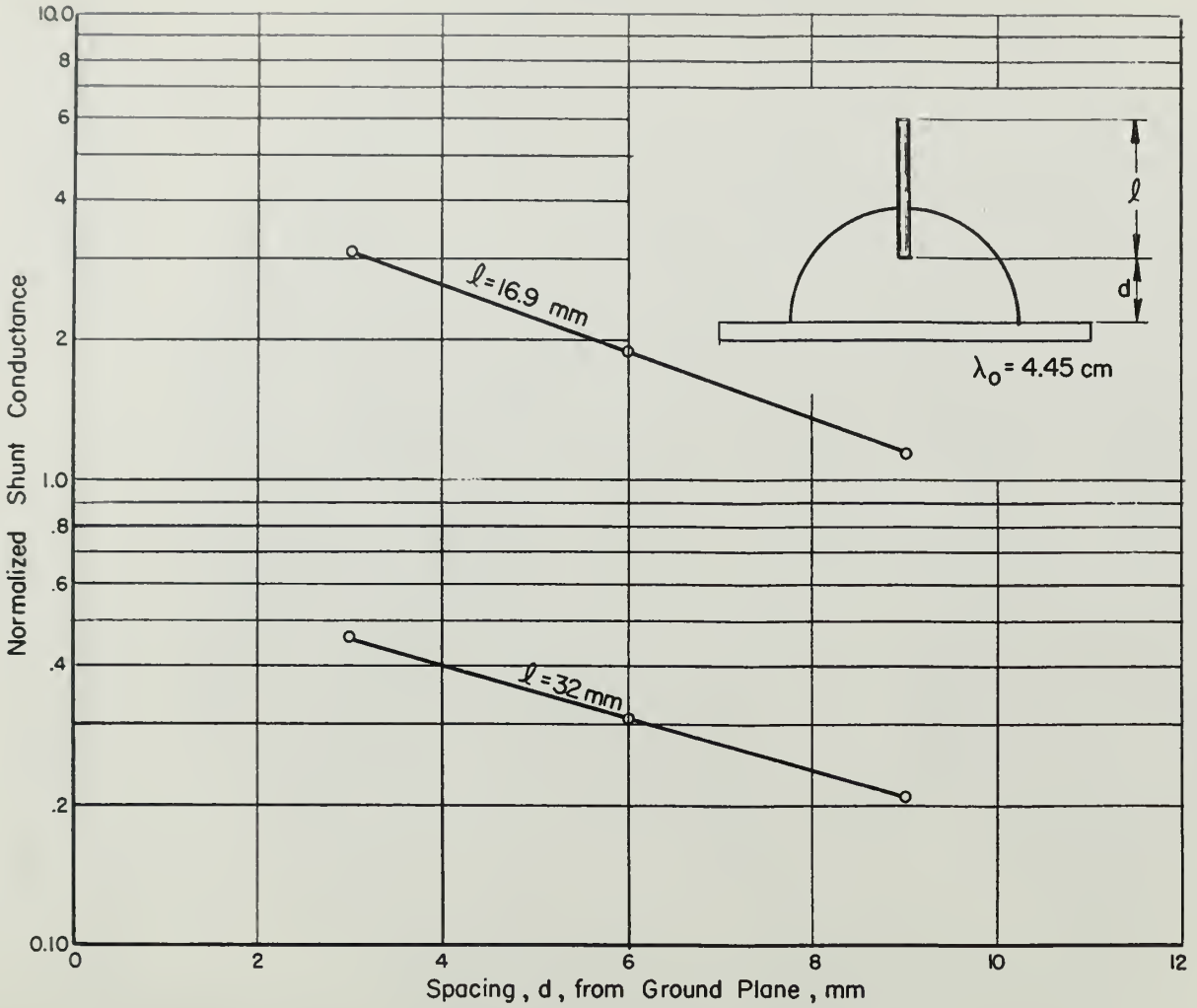

Figure 11. Normalized Shunt Conductance of Resonant Wires as a Function of the Spacing from the Ground Plane

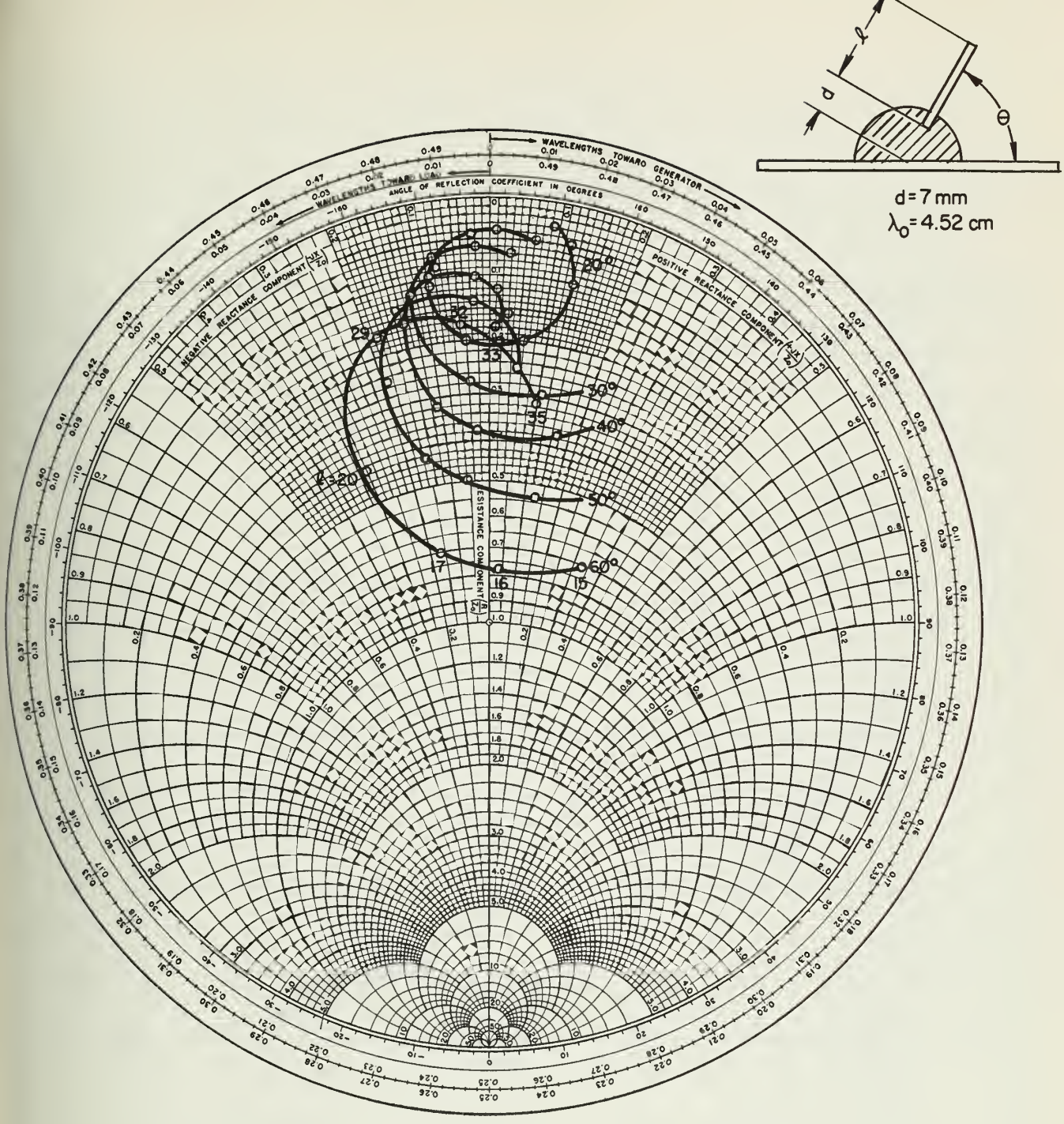

Figure 12. Shunt Admittance of an Inclined Wire as a Function of the Wire Length

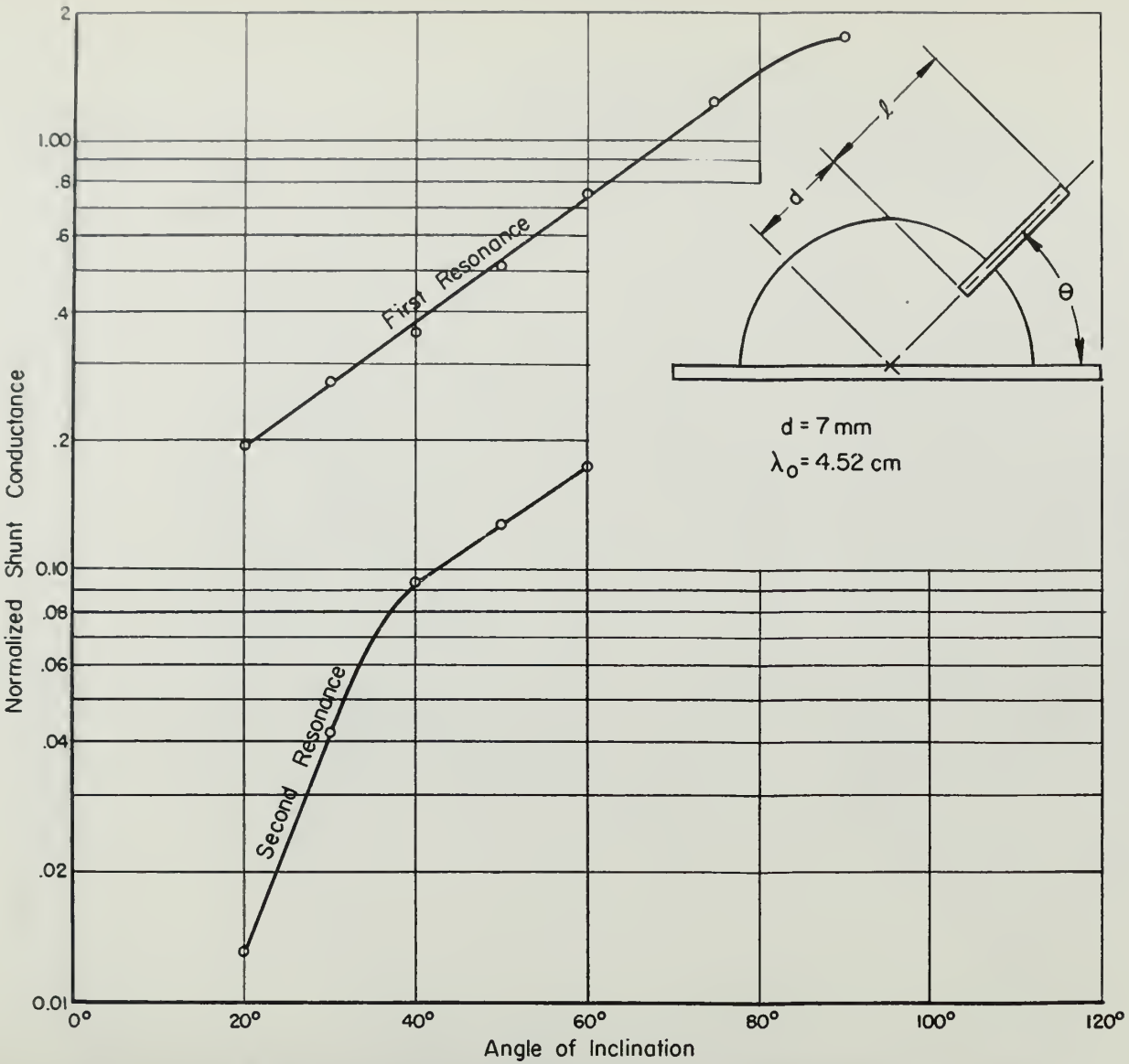

Figure 13. Normalized Shunt Conductance of a Resonant Wire as a Function of the Angle of Inclination

angle of inclination. It may be seen from the curve for the second resonance that a wide range of small conductances may be obtained.

Since only a single element was used, the measurements are not accurate for the second resonance curve for angles of 30° or less. For accurate results, several elements in tandem should be measured, as is done for loosely coupled slots in rectangular waveguides. This technique has the added advantage that it takes into account the incremental conductance due to the mutual coupling of the elements. It was found that the resonant length of the wire changed slightly with the angle of inclination, as is illustrated in Fig. 14.

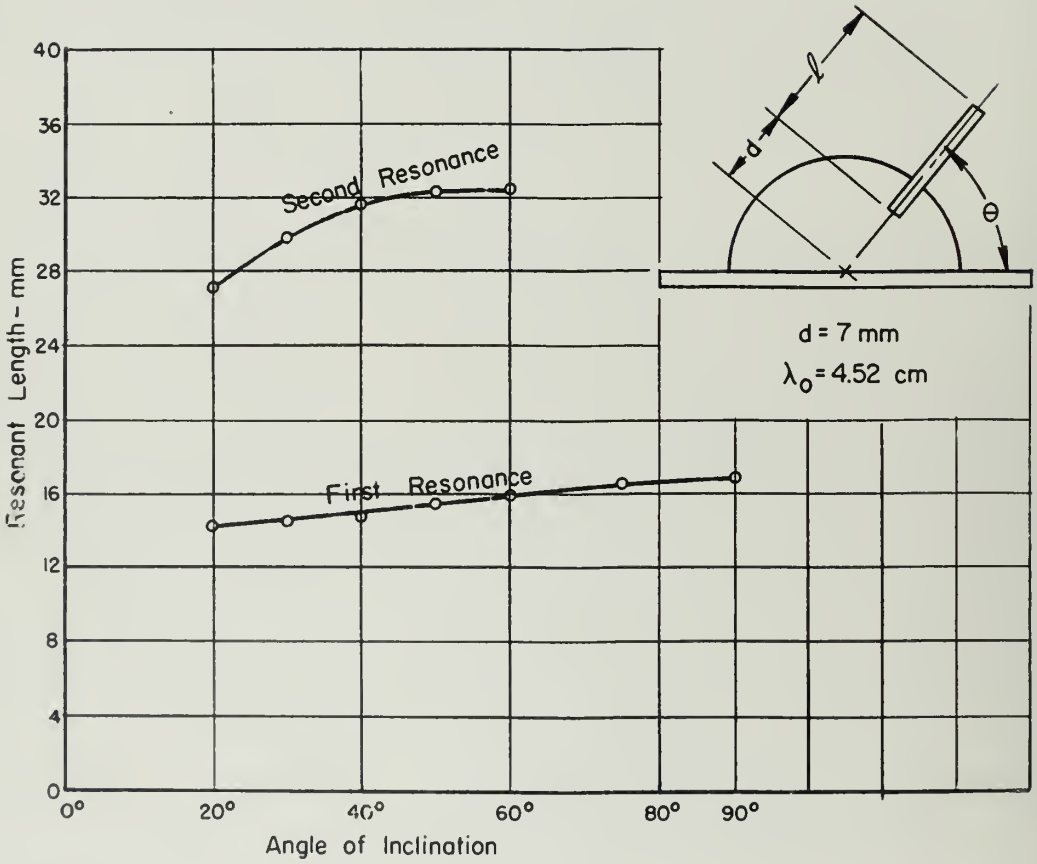

Figure 14. Length of Resonant Wire as a Function of the Angle of Inclination

4. ARRAY DESIGNS AND RESULTS

Since the inclined wire had the most desirable properties of the obstacles tested, it was used in the design of the arrays to be described. Now, given a prescribed pattern, the conventional linear array synthesis methods may be used to determine the array length, element spacings, and the equivalent shunt conductance of the antenna elements. Then, using Figs. 13 and 14, the angle θ and the wire length may be determined for each element. Two arrays which were designed by this procedure are shown in the photograph of Fig. 15. The

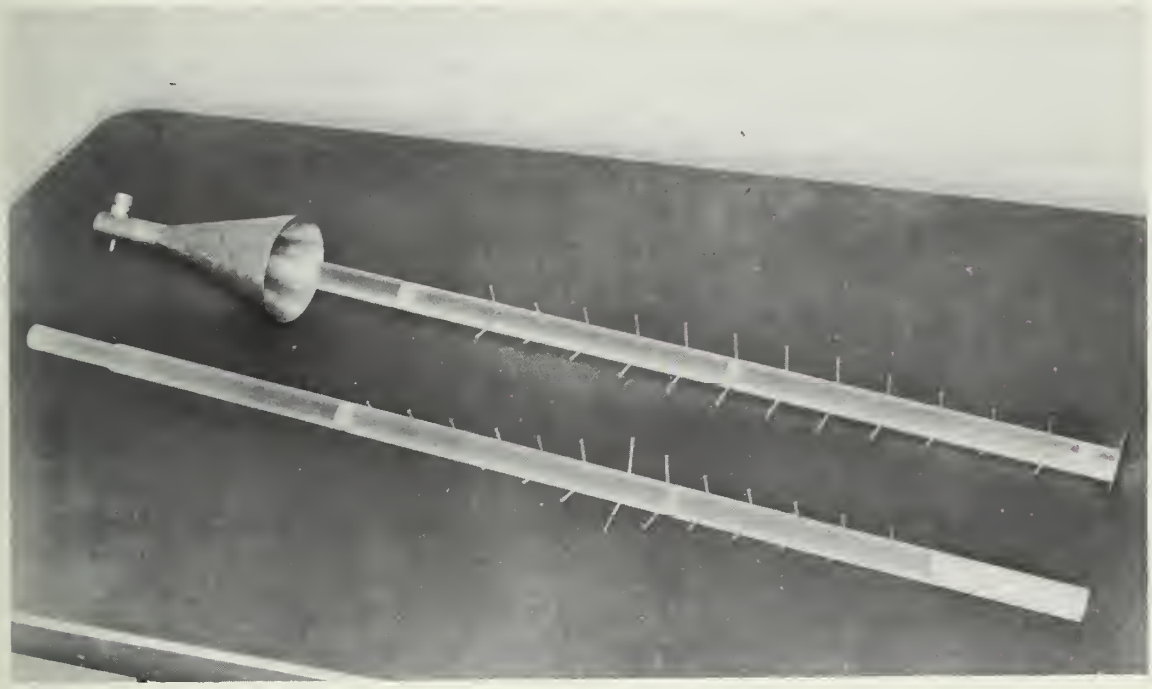

Figure 15. The Dolph-Tchebycheff and Cosecant Arrays

upper array is a 20 db Dolph-Tchebycheff broadside array and the lower is designed to produce a cosecant pattern. Notice that for the complete rod the image wire has been added so that each element consists of two wires with an included angle of 2θ. The horn feed wire is oriented so that the electric field of the HE_{11} mode is normal to the plane bisecting the angle between the wires. For the Tchebycheff array a two inch diameter short circuit plate proved quite satisfactory. For the lower non-resonant array a resistance card was inserted in the rod to form a matched load.

The radiation patterns which are presented below represent a first attempt. That is, the array was designed from Figs. 13 and 14, constructed, and tested without any adjustments being made. Since conventional methods have been used, little will be said about the method of design for the various types of arrays.

First consider the pattern in Fig. 16 of the uniform array with 12 identical elements at guide wavelength spacing. The pattern was measured in the longitudinal plane which bisects the angle between the wires. The beam width and sidelobe levels are very close to the theoretical values. The small lobe pointing towards the top of the figure represents the stray radiation from the horn exciter. A similar pattern was obtained with a similar array for which the half angle between the wires was 60° instead of 40°. The transverse radiation patterns for the two arrays are shown in Fig. 17. It will be noticed that the patterns for the two cases are considerably different. Theoretically, the patterns should be symmetrical about a vertical line. The discrepancy is due to a misalignment of the feed horn and slight variations in the wire length and inclination. Aside from the asymmetry the transverse patterns are probably not suitable for practical applications. However, it is felt that further experimentation would lead to antenna elements with various types of useful transverse patterns.

The design data and radiation pattern for the 20 db Dolph-Tchebycheff broadside array for 12 elements with guide wavelength spacing are shown in Fig. 18. The element conductances were made proportional to the square of the calculated excitation coefficients of the array. Note the excellent agreement between the predicted and measured side lobe level. The variation of the angle between the wires is readily apparent in the photograph of Fig. 19.

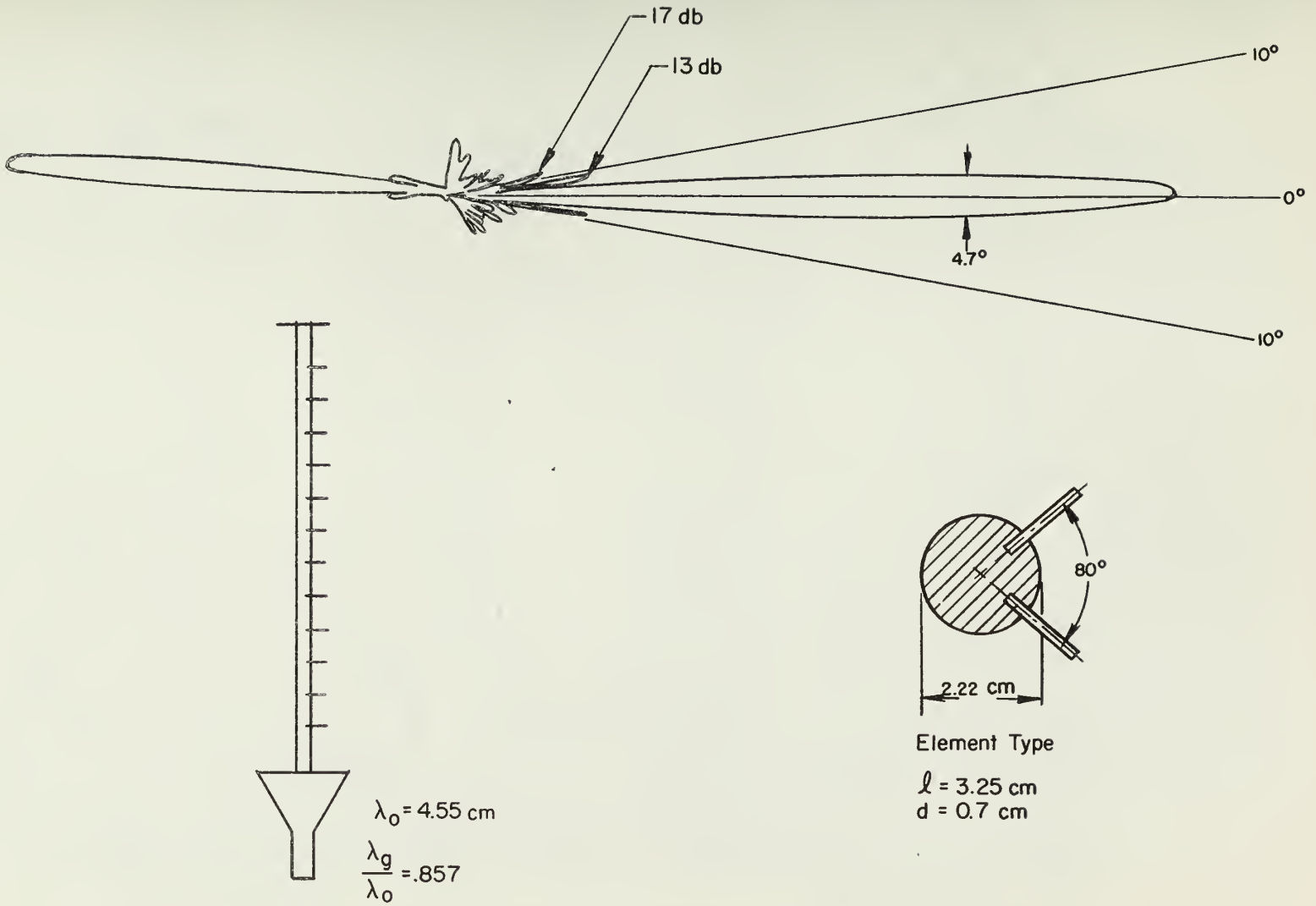

Figure 16. Radiation Pattern of a Uniform Broadside Array with 12 Elements at Guide Wavelength Spacing

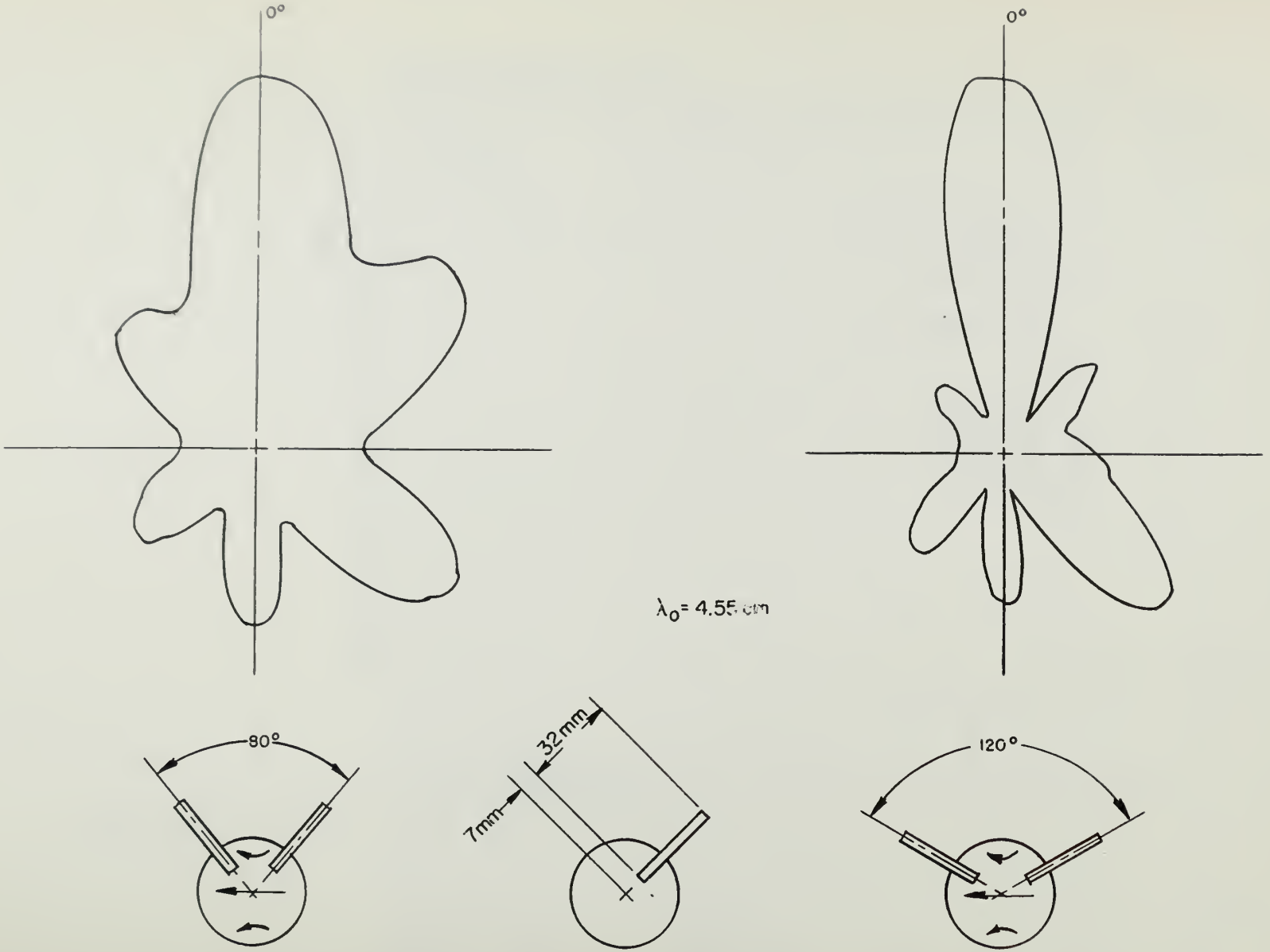

Figure 17. Transverse Radiation Patterns for Uniform Arrays

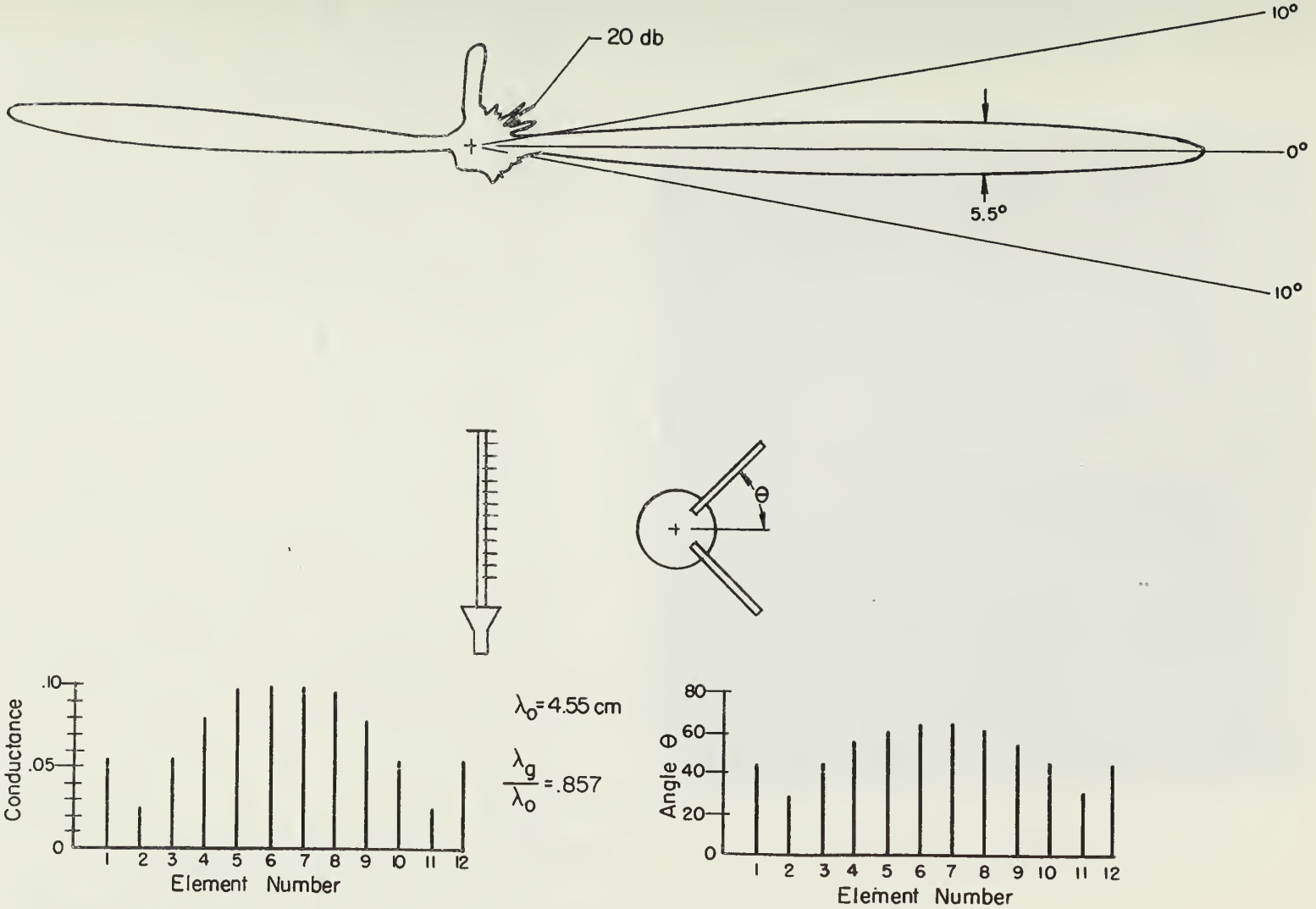

Figure 18. Radiation of a 20 db Dolph-Tchebycheff Broadside Array for 12 Elements with Guide Wavelength Spacing

Figure 19. An End View of the Dolph-Tchebycheff Array

Similar data are presented in Fig. 20 for a non-resonant uniform array of 12 elements with an element spacing of 0.75 λ_g. Since the purpose of this work has been to illustrate the method of design rather than to develop a practical antenna, the array was designed so that 40% of the input power to the array was absorbed in the matched resistance card termination on the dielectric rod. This simplifies the design calculations considerably for a short array since the VSWR along the line may be considered to be unity for design purposes. Larger array efficiencies could be obtained by a more refined design procedure. The direction of the beam and the beam width are in excellent agreement with the theoretical values. However the first side lobe is only 10 db down instead of 13 db down and the stray radiation from the horn is at a higher level than before. This latter effect is due to the reduction of the antenna gain which results from the absorbtion of power in the matched load.

The final example is for a non-resonant array designed to produce a cosecant pattern. The desired aperture distribution shown in

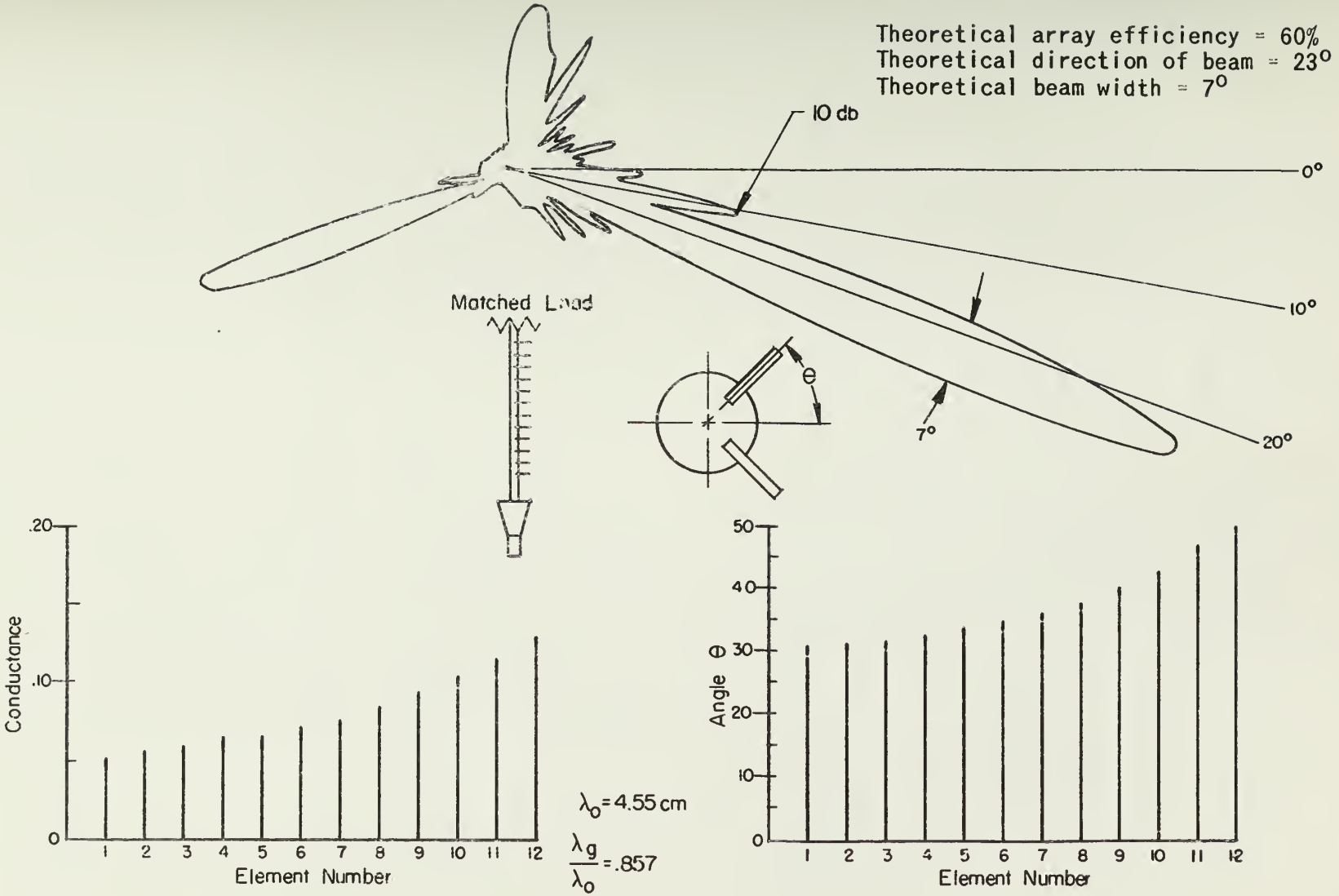

Figure 20. Radiation Pattern of a Nonresonant Uniform Array with 12 Elements with an Element Spacing of 0.75 λ_g

Fig. 21 was determined by Woodward's Method.[3] The parameter z represents distance along the array. The element locations were determined from the intersection of the curve for the desired aperture phase and the curve of the phase on the dielectric rod. The relative power to be radiated from each element was then determined from the curve of the desired power distribution in the aperture. Although this is an approximate design procedure, previous work had indicated that it was accurate when the element spacing was less than one wavelength. The above information was then used to determine the design data given in Fig. 22. It will be noticed that there is poor agreement between the predicted and experimental patterns. This difference is probably due to the wide variation of the angle (from 19^{o} to 60^{o}) between the wires. That is, it has been assumed in the design method that all the element patterns are identical. This is certainly not true for this case. In fact, it is rather surprising that the agreement for the two previous designs was so good since there was considerable variation of the angle between the wires for those cases.

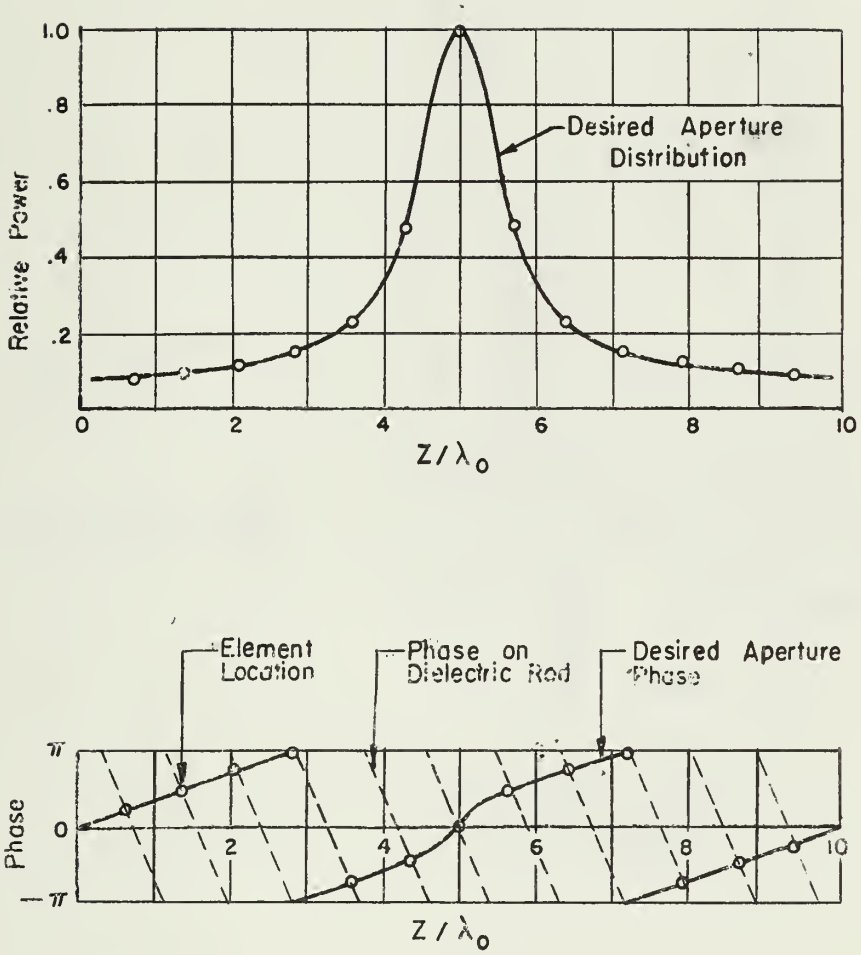

Figure 21. Design Curves for a Cosecant Pattern

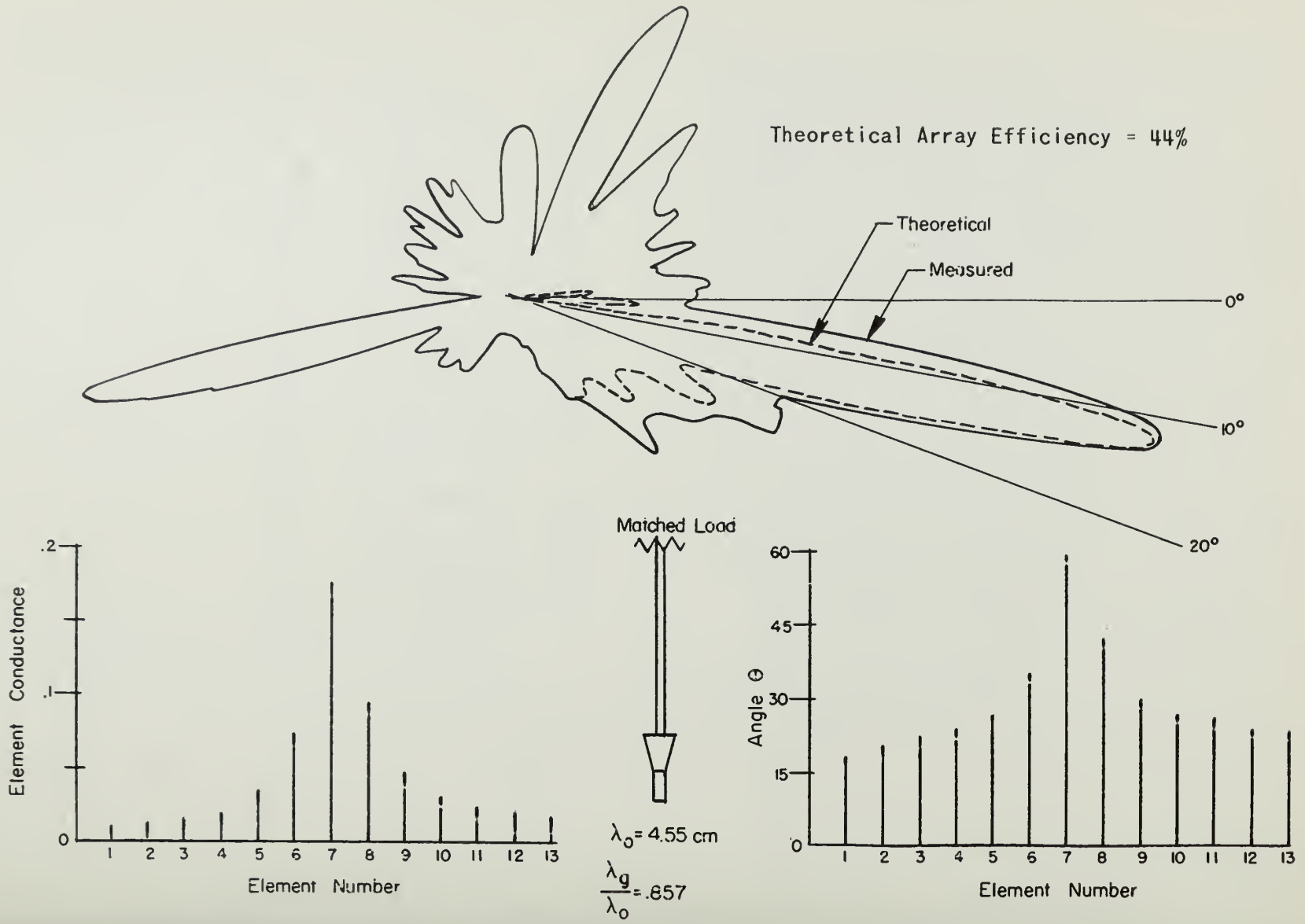

Figure 22 Radiation Pattern of a 13-Element Array Designed to Produce a Cosecant Pattern

5. SURFACE WAVE EXCITERS

There has been considerable interest recently in the surface wave excitation efficiency of various types of sources. The launching efficiency, η, of a source is defined as the ratio of the power converted to the desired surface wave to the sum of the radiated power and the surface wave power. The sources usually consist of large horns which have fairly high efficiencies. However, the usefulness of surface waveguides would be increased many times if simple and small, but efficient, exciters were available. Recent theoretical results have predicted efficiencies of 95% for a uniform current loop around a dielectric rod and for a line source above a grounded dielectric slab. However, experimental verification of these predictions is lacking.

The admittance measurements which were made for the transverse rings, wires, and slots may be used to calculate the efficiency of these obstacles when used as sources. Considering the rings and wires as sources on a semi-infinite line, it may be shown that the equivalent transmission line representation of the obstacle and rod waveguide is that of Fig. 23 where Z is the normalized shunt impedance of the obstacle. It has been assumed that a short circuit has been placed to the

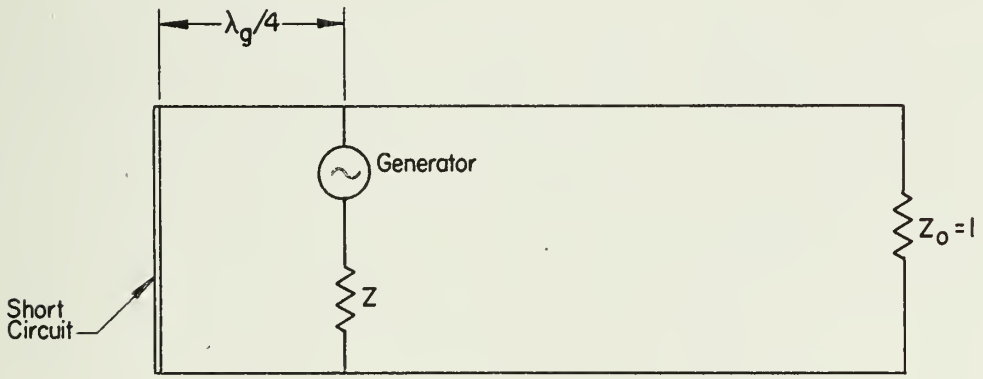

Figure 23. Equivalent Transmission Line Representation of a Transverse Ring or Wire Acting as a Source on the Rod Waveguide

left of the source. If the short circuit is placed a quarter wavelength from the source, then a simple calculation yields

$$\eta_{wire} = \frac{1}{1 + \text{Re } Z} \times 100 \text{ in percent.}$$

The impedance Z is identical to the passive shunt impedance that the obstacle presents to the surface waveguide with the generator terminals shorted, provided that the current distribution on the obstacle is the same for the sink and source conditions. This assumption should be accurate for obstacles which are small compared to a wavelength. In a similar manner, the equivalent transmission line representation for a transverse slot is a generator in parallel with the normalized shunt admittance of the slot. Thus for a slot the efficiency relation is

$$\eta_{slot} = \frac{1}{1 + \mathrm{Re}\ Y} \times 100 \text{ in percent.}$$

These expressions were used to compute the efficiency curves shown in Fig. 24. The ring appears to be the most efficient exciter (with an efficiency of 85%) of the obstacles which were considered as sources. By placing several rings at half-wavelength intervals on the line it should be possible to realize efficiencies of 95% or more. A detailed analysis which yields the above efficiency formulae and an experimental investigation of obstacle launching efficiency will be the subject of a subsequent technical report.

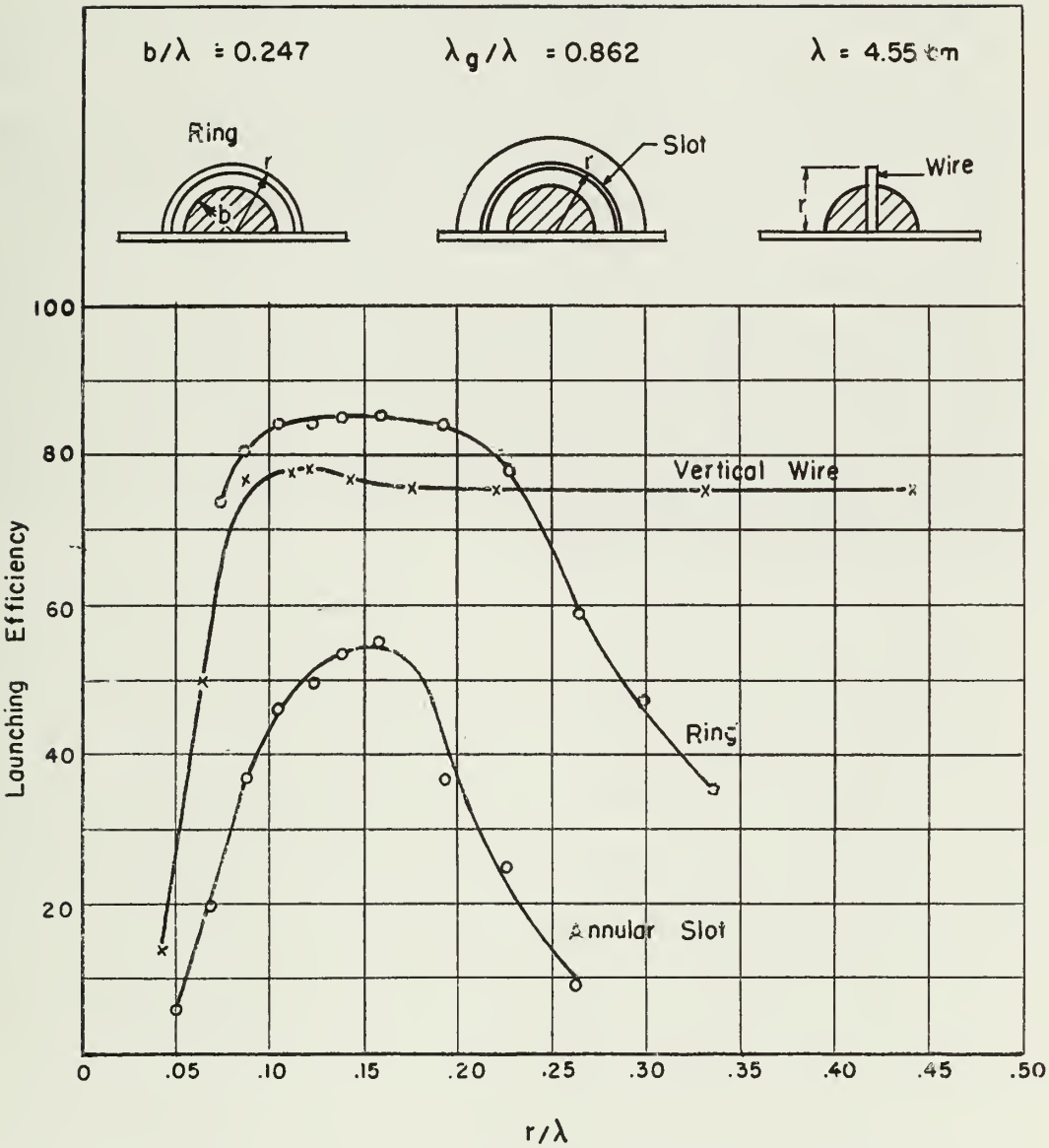

Figure 24. Launching Efficiency of a Ring, Annular Slot, and Vertical Wire.

6. CONCLUSIONS

The measurements have proven the feasibility of obtaining accurate control of the radiation from a dielectric rod waveguide in the longitudinal plane by means of placing obstacles along the waveguide. Since only a few types of obstacles have been investigated, it is likely that considerable control of the pattern in the transverse plane may be obtained by utilizing other types of obstacles such as dielectric pins, holes, or slots in the rod, and more suitable arrangements of intersecting wires. It should be possible to apply the same technique to other types of surface waveguides with equal success. The basic requirements needed for applying the design procedure are the following: an efficient surface wave exciter, the existence of only a single mode on the surface waveguide, an accurate means of determining the equivalent network for the coupling of the obstacle to the surface waveguide, and, of course, the discovery of obstacles for which the coupling may be varied over a wide range with only a moderate effect on the individual obstacle pattern. Conventional array design methods may then be used to obtain various types of patterns.

7. BIBLIOGRAPHY

1. Mueller, G. E. "A Broadside Dielectric Antenna," *Proc. I.R.E., Vol. 40,* pp. 71-75, January 1952.

2. Beam, R. E. *Final Report on Investigation of Multi-mode Propagation in Waveguides and Microwave Optics,* Army Signal Corps Contract No. W36-039 sc-38240, Microwave Laboratory, Northwestern University, Evanston, Illinois. 1 May 1949 to 30 November 1950.

3. Woodward, P. M. "A Method of Calculating the Field Over a Plane Aperture Required to Produce a Given Polar Diagram," *J.I.E.E., Part IIIA, Vol. 93,* pp. 1554-1558, March-May 1946.

DISTRIBUTION LIST FOR REPORTS ISSUED UNDER CONTRACT AF33(616)-3220

One copy each unless otherwise indicated.

Contractor
Wright Air Development Center
Wright-Patterson Air Force Base, Ohio

Attn: Mr. E.M. Turner, WCLRS-6
4 copies

Commander
Wright Air Development Center
Wright-Patterson Air Force Base, Ohio

Attn: Mr. N. Draganjac, WCLNT-4

Armed Services Technical Information
Knott Building Agency
4th and Main Streets 5 copies
Dayton 2, Ohio 1 repro.

Attn: DSC SA(Reference AFR205-43)

Commander
Hq. A.F. Cambridge Research Center
Air Research and Development Command
Laurence G. Hanscom Field
Bedford, Massachusetts

Commander
Hq A.F. Cambridge Research Center
Air Research and Development Command
Laurence G Hanscom Field
Bedford, Massachusetts

Attn: CRTOTL-1

Commander
Hq A.F. Cambridge Research Center
Air Research and Development Command
Laurence G Hanscom Field
Bedford, Massachusetts

Attn: CRRD, R E Hiatt

Air Force Development Field
Representative
Attn: Major M.N. Abramovich
Code 1110
Naval Research Laboratory
Washington 25, D. C.

Director
Ballistics Research Lab.
Aberdeen Proving Ground, Maryland

Attn: Ballistics Measurement Lab.

Office of the Chief Signal Officer
Attn: SIGNET-5
Eng. & Technical Division
Washington 25, D. C.

Commander
Rome Air Development Center
Attn: RCERA-1, D. Mather
Griffiss Air Force Base
Rome, New York

Director
Evans Signal Laboratory
Belmar, New Jersey

Attn: Mr. O. C. Woodyard

Director
Evans Signal Laboratory
Belmar, New Jersey

Attn: Mr. S Krevsky

Director
Evans Signal Laboratory
Belmar, New Jersey

Attn: Technical Document Center

Naval Air Missile Test Center
Point Mugu, California

Attn: Antenna Section

Commander
U.S. Naval Air Test Center
Attn: ET-315
Antenna Section
Patuxent River, Maryland

Commander
Air Force Missile Test Center
Patrick Air Force Base, Florida

Attn: Technical Library

Chief
BuShips, Room 3345
Department of the Navy
Attn: Mr. A. W. Andrews
Code 883
Washington 25, D. C.

Director
Naval Research Laboratory
Attn: Dr. J. I. Bohnert
Anocostia
Washington 25, D. C.

National Bureau of Standards
Department of Commerce
Attn: Dr. A. G. McNish
Washington 25, D. C.

Director
U.S. Navy Electronics Lab.
Attn: Dr. T. J. Keary
Code 230
Point Loma
San Diego 52, California

Chief of Naval Research
Department of the Navy
Attn Mr. Harry Harrison
Code 427, Room 2604
Bldg. T-3
Washington 25, D. C.

Airborne Instruments Lab., Inc.
Attn: Dr. E. G. Fubini
Antenna Section
160 Old Country Road
Mineola, New York
M/F Contract AF33(616)-2143

Andrew Alford Consulting Engrs.
Attn: Dr. A. Alford
299 Atlantic Ave.
Boston 10, Massachusetts
M/F Contract AF33(038)-23700

Chief
Bureau of Aeronautics
Department of the Navy
Attn: W. L. May, Aer-EL-4114
Washington 25, D. C.

Chance-Vought Aircraft Division
United Aircraft Corporation
Attn: Mr. F. N. Kickerman
Thru: BuAer Representative
Dallas, Texas

Consolidated-Vultee Aircraft Corp.
Attn: Dr. W. J. Schart
San Diego Division
San Diego 12, California
M/F Contract AF33(600)-26530

Consolidated-Vultee Aircraft Corp.
Fort Worth Division
Attn: C. R. Curnutt
Fort Worth, Texas
M/F Contract AF33(038)-21117

Textron American, Inc. Div.
Dalmo Victor Company
Attn: Mr. Glen Walters
1414 El Camino Real
San Carlos, California
M/F Contract AF33(038)-30525

Dorne & Margolin
30 Sylvester Street
Westbury
Long Island, New York
M/F Contract AF33(616)-2037

Douglas Aircraft Company, Inc.
Long Beach Plant
Attn: J. C. Buckwalter
Long Beach 1, California
M/F Contract AF33(600)-25669

Electronics Research, Inc.
2300 N. New York Avenue
P. O. Box 327
Evansville 4, Indiana
M/F Contract AF33(616)-2113

DISTRIBUTION LIST (Cont.)

Beech Aircraft Corporation
Attn: Chief Engineer
6600 E. Central Avenue
Wichita 1, Kansas
M/F Contract AF33(600)-20910

Bell Aircraft Corporation
Attn: Mr. J. D. Shantz
Buffalo 5, New York
M/F Contract W-33(038)-14169

Boeing Airplane Company
Attn: G. L. Hollingsworth
7755 Marginal Way
Seattle, Washington
M/F Contract AF33(038)-21096

Grumman Aircraft Engineering Corp.
Attn: J. S. Erickson,
Chief Engineer
Bethpage
Long Island, New York
M/F Contract NOa(s) 51-116

Hallicrafters Corporation
Attn: Norman Foot
440 W. 5th Avenue
Chicago, Illinois
M/F Contract AF33(600)-26117

Hoffman Laboratories, Inc.
Attn: Markus McCoy
Los Angeles, California
M/F Contract AF33(600)-17529

Hughes Aircraft Corporation
Division of Hughes Tool Company
Attn: Dr. Vanatta
Florence Avenue at Teale
Culver City, California
M/F Contract AF33(600)-27615

Johns Hopkins University
Radiation Laboratory
Attn: Dr. D. D. King
1315 St. Paul Street
Baltimore 2, Maryland
M/F Contract AF33(616)-68

Fairchild Engine & Airplane Corp.
Fairchild Airplane Division
Attn: L. Fahnestock
Hagerstown, Maryland
M/F Contract AF33(038)-18499

Federal Telecommunications Lab.
Attn: Mr. A. Kandoian
500 Washington Avenue
Nutley 10, New Jersey
M/F Contract AF33(038)-13289

Glenn L. Martin Company
Attn: N. M. Voorhies
Baltimore 3, Maryland
M/F Contract AF33(600)-21703

Massachusetts Institute of Tech.
Attn: Prof. H. J. Zimmermann
Research Lab. of Electronics
Cambridge, Massachusetts
M/F Contract AF33(616)-2107

North American Aviation, Inc.
Aerophysics Laboratory
Attn: Dr. J. A. Marsh
12214 Lakewood Boulevard
Downey, California
M/F Contract AF33(038)-18319

North American Aviation, Inc.
Los Angeles International Airport
Attn: Mr. Dave Mason
Engineering Data Section
Los Angeles 45, California
M/F Contract AF33(038)-18319

Northrop Aircraft Incorporated
Attn: Northrop Library
Dept. 2135
Hawthorne, California
M/F Contract AF33(600)-22313

Ohio State Univ. Research Foundation
Attn: Dr. T. C. Tice
310 Administration Bldg.
Ohio State University
Columbus 10, Ohio
M/F Contract AF18(600)-85

Land-Air Incorporated
Cheyenne Division
Attn: Mr. B.L. Michaelson
Chief Engineer
Cheyenne, Wyoming
M/F Contract AF33(600)-22964

Lockheed Aircraft Corporation
Attn: C. L. Johnson
P. O. Box 55
Burbank, California
M/F NOa(S)-52-763

McDonnell Aircraft Corporation
Attn: Engineering Library
Lambert Municipal Airport
St. Louis 21, Missouri
M/F Contract AF33(600)-8743

Michigan, University of
Aeronautical Research Center
Attn: Dr. R.D. O'Neill
Willow Run Airport
Ypsilanti, Michigan
M/F Contract AF33(038)-21573

Chief
Bureau of Ordnance
Department of the Navy
Attn: A.D. Bartelt
Washington 25, D. C.

Radioplane Company
Van Nuys, California
M/F Contract AF33(600)-23893

Raytheon Manufacturing Company
Attn: Dr. H.L. Thomas
Documents Section
Waltham 54, Massachusetts
M/F Contract AF33(038)-13677

Republic Aviation Corporation
Attn: Engineering Library
Farmingdale
Long Island, New York
M/F Contract AF33(038)-14810

Ryan Aeronautical Company
Lindbergh Drive
San Diego 12, California
M/F Contract W-33(038)-ac-21370

Sperry Gyroscope Company
Attn: Mr. B. Berkowitz
Great Neck
Long Island, New York
M/F Contract AF33(038)-14524

Temco Aircraft Corp.
Attn: Antenna Design Group
Dallas, Texas
M/F Contract AF33(600)-31714